ORIGINAL ARTICLE

Journal of Cachexia, Sarcopenia and Muscle 2023; **14**: 1454–1467
Published online 13 April 2023 in Wiley Online Library (wileyonlinelibrary.com) **DOI:** 10.1002/jcsm.13233

Identification of Ubr1 as an amino acid sensor of steatosis in liver and muscle

Wanni Zhao[1], Yansong Zhang[2*], Siyuan Lin[2,3], Yajuan Li[2], Alan Jian Zhu[2,4], Hanping Shi[1*] & Min Liu[2,4*]

[1]*Department of Gastrointestinal Surgery/Clinical Nutrition, Key Laboratory of Cancer FSMP for State Market Regulation, Beijing Shijitan Hospital, Capital Medical University, Beijing, China;* [2]*Ministry of Education Key Laboratory of Cell Proliferation and Differentiation, School of Life Sciences, Peking University, Beijing, China;* [3]*Tsinghua-Peking Center for Life Sciences, Tsinghua University, Beijing, China;* [4]*Peking-Tsinghua Center for Life Sciences, Academy for Advanced Interdisciplinary Studies, Peking University, Beijing, China*

Abstract

Background Malnutrition is implicated in human metabolic disorders, including hepatic steatosis and myosteatosis. The corresponding nutrient signals and sensors as well as signalling pathways have not yet been well studied. This study aimed to unravel the nutrient-sensing mechanisms in the pathogenesis of steatosis.

Methods Plin2, a lipid droplet (LD) protein-inhibiting lipolysis, is associated with steatosis in liver and muscle. Taking advantage of the Gal4-UAS system, we used the *Drosophila melanogaster* wing imaginal disc as an in vivo model to study the regulation of Plin2 proteostasis and LD homeostasis. *Drosophila* Schneider 2 (S2) cells were used for western blotting, immunoprecipitation assays, amino acid-binding assays and ubiquitination assays to further investigate the regulatory mechanisms of Plin2 in response to nutrient signals. Mouse AML12 hepatocytes, human JHH-7 and SNU-475 hepatoma cells were used for immunofluorescence, western blotting and immunoprecipitation to demonstrate that the mode of Plin2 regulation is evolutionarily conserved. In addition, we purified proteins from HEK293 cells and reconstituted in vitro cell-free systems in amino acid-binding assays, pulldown assays and ubiquitination assays to directly demonstrate the molecular mechanism by which Ubr1 senses amino acids to regulate Plin2 proteostasis.

Results As a lipolysis inhibitor, Plin2 was significantly elevated in liver ($P < 0.05$) and muscle ($P < 0.05$) in patients with steatosis. Consistently, we found that the ubiquitin moiety can be conjugated to any Lys residue in Plin2, ensuring robust clearance of Plin2 by protein degradation. We further demonstrated that the E3 ubiquitin ligase Ubr1 targets Plin2 for degradation in an amino acid-dependent manner. Ubr1 uses two canonical substrate-binding pockets, independent of each other, to bind basic and bulky hydrophobic amino acids, respectively. Mechanistically, amino acid binding allosterically activates Ubr1 by alleviating Ubr1's auto-inhibition. In the absence of amino acids, or when the amino acid-binding capacity of Ubr1 is diminished, Ubr1-mediated Plin2 degradation is inactivated, leading to steatosis.

Conclusions We identified Ubr1 as an amino acid sensor regulating Plin2 proteostasis, bridging the knowledge gap between steatosis and nutrient sensing. Our work may provide new strategies for the prevention and treatment of steatosis.

Keywords Amino acid; Degradation; Hepatic steatosis; Lipid droplet; Myosteatosis; Plin2; Ubiquitination; Ubr1

Received: 9 August 2022; Revised: 23 January 2023; Accepted: 15 March 2023
**Correspondence to: Yansong Zhang, Ministry of Education Key Laboratory of Cell Proliferation and Differentiation, School of Life Sciences, Peking University, Beijing 100871, China. Email: zhangyansong@pku.edu.cn;*
Hanping Shi, Department of Gastrointestinal Surgery/Clinical Nutrition, Key Laboratory of Cancer FSMP for State Market Regulation, Beijing Shijitan Hospital, Capital Medical University, Beijing 100038, China. Email: shihp@ccmu.edu.cn;
Min Liu, Ministry of Education Key Laboratory of Cell Proliferation and Differentiation, School of Life Sciences, Peking University, Beijing 100871, China. Email: liumin02@pku.edu.cn
Wanni Zhao and Yansong Zhang are co-first authors.

Introduction

Nutrient sensing is pivotal for organisms to optimize their myriad of cellular metabolic processes.[1,2] Dysregulation of nutrient-sensing pathways often leads to a variety of human metabolic diseases, including obesity, hyperlipidaemia, type 2 diabetes and cancer.[2] Unravelling the underlying molecular mechanisms is a prerequisite for developing strategies for these unmet clinical needs. However, nutrient-sensing mechanisms remain largely unknown.[2]

Steatosis is a pathological condition characterized by excessive accumulation of lipid droplets (LDs) in non-adipose tissues, and its pathogenesis is commonly associated with abnormal nutrition status.[3] Hepatic steatosis, which can progress to non-alcoholic steatohepatitis (NASH) and cirrhosis over time, and myosteatosis, which develops into muscle atrophy and sarcopenia, occur mainly following nutrient overload.[3,4] Paradoxically, nutritional deficiencies can also lead to hepatic steatosis and myosteatosis.[5–7] As an extreme example, protein-energy malnourished children almost always have features of fatty liver and sarcopenia.[5,6] Similarly, patients with anorexia nervosa suffer from severe hepatic steatosis and muscle atrophy.[7,8] Moreover, people who lose weight quickly as a result of dieting have a higher risk of hepatic steatosis and myosteatosis.[5,7] These clinical observations led us to wonder whether a common nutrient-sensing mechanism might underlie this apparent paradox.

Ubr1 is the first E3 ubiquitin ligase identified to mediate the Arg/N-degron pathway.[9] Ubr1 uses its UBR-box-1 and UBR-box-2 domains to target N-terminal amino acid residues of protein substrates.[10,11] The UBR-box-1 domain specifically target three basic amino acid residues (Arg, His and Lys) at the N-terminus of protein substrates, whereas the UBR-box-2 domain is specific for five bulky hydrophobic amino acids (Ile, Leu, Phe, Trp and Tyr).[12] In this context, these N-terminal residues act as Arg/N-degrons, destabilizing protein substrates.[13] Our previous work has shown that amino acids can activate Ubr1 to degrade Plin2, an LD protein that protects LDs from association of lipases.[14] However, how amino acids activate Ubr1 and the role of Ubr1 in the pathogenesis of steatosis remain to be determined.

In this study, we identified Ubr1 as an amino acid sensor of steatosis, bridging the knowledge gap between nutrient sensing and LD homeostasis. Mechanistically, amino acid binding to UBR-box-1/2 domains activates Ubr1 by dissociating its auto-inhibitory domain from the Plin2-binding site. These findings may provide new strategies for the prevention and treatment of steatosis.

Material and methods

Amino acid-binding assays

For amino acid-binding assays, standard procedures were used to prepare amino acid-immobilized beads with some modifications.[15] Briefly, Silica MagBeads ($-NH_2$) (Aladdin, S8099) were incubated overnight at room temperature with Fmoc-β-Lys (Bidepharm, BD17410), Fmoc-β-Leu (Rhawn, R003672) or Fmoc-β-Ala (Adamas, 51341A) in DMF containing 1 mM EDC and 1 mM HOBt. The beads were then washed in DMF and incubated in 150 mM acetic anhydride in DMF for 30 min at room temperature to block unreacted $-NH_2$ groups. These Fmoc amino acid-conjugated beads were further washed in DMF and incubated in 50% DBU for 2 h to remove the Fmoc group. The amino acid-immobilized beads were stored in methanol at 4°C. Purified Ubr1 proteins or amino acid starved cell lysates were supplemented with washed Lys-immobilized, Leu-immobilized or Ala-immobilized beads and rotated overnight at 4°C. Immunoprecipitates were then washed three times with RIPA lysis buffer and analysed by Western blotting. For competition, free amino acids were added to cell lysates at a final concentration of 1 mM.

Antibodies

The antibodies used in this study are listed as follows: mouse anti-FLAG (1:3,000; Engibody Biotechnology; AT0022), mouse anti-HA tag (1:2,000; 6E2; Cell Signaling Technology [CST]; 2367S), mouse anti-Myc tag (1:2,000; 9B11; CST; 2276S), rabbit anti-GFP (1:4,000), rabbit anti-β-actin (1:1,000; ABclonal; AC026), rabbit anti-UBR1 (1:1,000; Proteintech; 26069-1-AP) for human UBR1 and mouse Ubr1, rabbit anti-UBR2 (1:1,000; Affinity Biosciences; DF9491) for human UBR2 and mouse Ubr2, rabbit anti-PLIN2 (1:2,000; Abcam; ab108323) for human PLIN2, rabbit anti-Plin2 (1:2,000; Abcam; ab52356) for mouse Plin2, and rabbit anti-Ubr1 (1:2,000) for fly Ubr1.[14]

Cell culture, transfection and drug treatment

Drosophila Schneider 2 (S2) cells (American type culture collection [ATCC], CRL-1963) were cultured at 25°C in *Drosophila* Schneider's medium (Thermo Fisher, 21720024) containing 10% fetal bovine serum (FBS) (Lanzhou Bailing Biotechnology, 20130507) and 100 mg/mL penicillin/streptomycin (Thermo Fisher, 15140122). Transfection was per-

DOI: 10.1002/jcsm.13233

formed using the calcium phosphate method as previously described.[16]

Mouse AML12 hepatocytes (ATCC, CRL-2254) and human JHH-7 hepatoma cells (Japanese Cancer Research Resources Bank, JCRB-1031) were cultured at 37°C with 5% CO_2 in Dulbecco's modified Eagle's medium (Thermo Fisher, 21720024) containing 10% FBS and 100 mg/mL penicillin/streptomycin. Human SNU-475 hepatoma cells (ATCC, CRL-2236) were cultured at 37°C with 5% CO_2 in Roswell Park Memorial Institute 1640 medium (Thermo Fisher, 11875101) containing 10% FBS and 100 mg/mL penicillin/streptomycin.

For amino acid starvation treatment of S2 cells, cells were incubated with Krebs–Ringer bicarbonate buffer (KRB, 5.4 mM calcium chloride, 0.7 mM dibasic sodium phosphate, 10 mM glucose, 0.5 mM magnesium chloride, 1.5 mM monobasic sodium phosphate, 4.52 mM potassium chloride, 15 mM sodium bicarbonate, 120.7 mM sodium chloride, pH 7.4) for 60 min.[17] For refeeding treatment, amino acid-starved S2 cells were incubated with Schneider's medium for 10 min. For starvation treatment of mouse AML12 hepatocytes, human JHH-7 and SNU-475 hepatoma cells, cells were washed once with PBS and then cultured in media lacking either glucose (glucose starvation), amino acids (amino acid starvation) or both (glucose & amino acid starvation) for 4 h. For refeeding treatment, starved cells were incubated with full culture media for 30 minutes.

Pulse-chase experiments were performed using standard protocols as previously described.[14] Briefly, *Drosophila* S2 cells were transfected with pMT plasmids expressing HA-tagged $Plin2^{KR}$ or $Plin2^{KR}$ variants, and incubated in Schneider's medium supplemented with 1 mM $CuSO_4$ (Sigma-Aldrich, C1297) for 12 h to induce protein production (i.e. pulse). After $CuSO_4$ was removed, cells were incubated in Schneider's medium containing cycloheximide (CHX, 50 μg/mL, Sigma-Aldrich, 5087390001), a translation elongation inhibitor used to block nascent protein synthesis (i.e. chase). Four hours later, S2 cells were harvested for western blotting.

Fly genetics

Fly culture and crosses were performed according to standard procedures.[16] Fly stocks used in this study are listed as follows: *ap*-Gal4 (Bloomington Drosophila Stock Center [BDSC]; 3041); UAS-*myr-mRFP* (BDSC; 7718); UAS-*w*-RNAi (Tsinghua Fly Center; THU0583); UAS-*Ubc6*-RNAi (Vienna Drosophila Resource Center [VDRC]; 23230); UAS-*Ubr1*-RNAi (BDSC; 31374). See *Table* S1 for detailed genotypes and experimental conditions.

Immunoprecipitation and western blotting

Western blotting analyses were performed using standard protocols.[16] Cells were lysed in RIPA lysis buffer [50 mM Tris–HCl (Sigma-Aldrich, T1530), 150 mM NaCl, 1% NP-40 (Sigma-Aldrich, I8896), 0.1% SDS, 0.5% sodium deoxycholate (Sigma-Aldrich, D6750), pH 8.0] supplemented with EDTA-free protease inhibitor cocktail (Roche, 13538100).

For immunoprecipitation, cells were plated in six-well plates and transfected with transgene expressing vectors. Forty-eight hours after transfection, cells were harvested and lysed in RIPA lysis buffer containing protease inhibitor at 4°C for 30 min. To inhibit protein degradation in the proteasome, cells were incubated with cultured medium containing 20 μM MG132 for 6 h as indicated. After centrifugation, supernatants of cell lysates were supplemented with washed FLAG (Sigma-Aldrich, A2220) or Myc antibody-conjugated agarose (Thermo Fisher, 20169) and rotated at 4°C for 12 h. Immunoprecipitates were then washed in triplicates with RIPA lysis buffer and analysed by western blotting. For immunoprecipitation of endogenous PLIN2, multiple rounds of centrifugation were conducted to remove insoluble components in cell extracts. Supernatants were first incubated at 4°C with anti-PLIN2 or anti-Plin2 antibody for 12 h, followed by an additional 8 h with protein A/G beads (Thermo Fisher, 10006D/10007D).

In vivo and in vitro ubiquitination analyses

For in vivo ubiquitination assay, hot lysis-extracted protein lysates were prepared as previously described.[16] Briefly, S2 cells were incubated with Schneider's medium containing 20 μM MG132 for 6–8 h to prevent degradation of ubiquitinated proteins. Harvested cells were resuspended in denaturing buffer (50 mM Tris–HCl, 0.5 mM EDTA, 1% SDS, pH 7.5) supplemented with protease inhibitors and boiled for 5 min to eliminate non-covalently bound proteins. After centrifugation, supernatants were diluted 1:3 with RIPA lysis buffer to reduce the SDS concentration. Diluted supernatants were subjected to immunoprecipitation followed by western blotting.

For *in vitro* ubiquitination assay, 2 μg purified FLAG-Plin2 protein was incubated with 15 μg ubiquitin, 550 ng UBE1 (E1 ubiquitin-activating enzyme), 850 ng HR2B (E2 ubiquitin-conjugating enzyme) and 2 μg purified Ubr1 proteins, with or without amino acids in 1× ubiquitin reaction buffer containing 12.5 mM Mg-ATP at 37°C for 60 min. Protein purification was performed using standard protocols as previously described.[18]

Reactions were terminated by boiling in SDS-loading buffer for 5 min and analysed by western blotting.

Lipid staining, in situ hybridization and immunofluorescence

Lipid staining of third-instar larval wing imaginal discs was performed as previously described.[19] Briefly, wing imaginal discs dissected from third-instar larvae were fixed in 4% paraformaldehyde for 15 min, washed three times with PBS buffer and incubated with PBS buffer containing 0.05 mg/mL Nile red (Sigma-Aldrich, 72485) for 10 min before mounting in VECTASHIELD Antifade Mounting Medium (Vector Laboratories; H-1200).

In situ hybridization was performed following standard protocols, as previously described.[16] Briefly, third-instar larval wing imaginal discs with the corresponding genotype were dissected, fixed, dehydrated, rehydrated and incubated overnight at 65°C with *Ubr1* or *Ubc6* RNA probes synthesized using a Digoxigenin RNA Labeling Kit (Roche; 11175025910). Discs were washed 7–10 times with PBSTw buffer (PBS containing 0.1% Tween-20, Sigma-Aldrich, P1379) at 65°C, then incubated with HRP-conjugated anti-DIG antibody overnight at 4°C. The signal was further amplified using the TSA Plus Fluorescence Kit (PerkinElmer, NEL741001KT) at room temperature. Primers used for generating RNA probes are listed in *Table* S2.

For immunofluorescence staining of mouse AML12 hepatocytes, standard procedure was used as previously described.[16] Briefly, cells cultured on poly-L-lysine-coated coverslips in 6-well or 24-well plates were fixed in 4% paraformaldehyde for 15 min at room temperature, washed with PBSTr buffer (PBS plus 0.1% Triton X-100, Sigma-Aldrich, T8787) and then incubated overnight with anti-Plin2 antibody at 4°C. After three washes with PBSTr buffer, cells were incubated with secondary antibody for 2 h at room temperature and washed three times with PBSTr buffer. Cells were incubated with PBS buffer containing 0.01 mg/mL DAPI (Thermo Fisher, 62248) and 2 μM BODIPY (Thermo Fisher, D3922) for 5 min before mounting in VECTASHIELD Antifade Mounting Medium. To quantify the fluorescence intensity of Plin2 or BODIPY in cells, images were taken with the same confocal set-up. The NIH ImageJ software was used to measure fluorescence intensity based on the mean pixel intensity. Each dot represents fluorescence intensity of an image field.

Fluorescence images were acquired with a Leica TCS SP8 confocal system using a 20× objective (Leica Microsystems; https://www.leica-microsystems.com). Minor image adjustments (brightness and/or contrast) were performed in Adobe Photoshop CS5 (Adobe; https://www.adobe.com/cn/products/photoshop.html). Figures were assembled in Adobe Illustrator CC (Adobe; https://www.adobe.com/cn/products/illustrator.html).

Microarray data analyses

For microarray data analyses, we searched the GEO DataSets database (https://www.ncbi.nlm.nih.gov/geo/) using the keyword 'steatosis geo accession' and downloaded the gene expression profiles of GSE138312 and GSE167186.[20,21] The platform for GSE138312 is GPL21290 (Illumina HiSeq 3000), which includes 13 liver samples from patients with hepatic steatosis and 14 liver samples from individuals without steatosis. The platforms for GSE167186 are GPL20301 (Illumina HiSeq 4000) and GPL24676 (Illumina NovaSeq 6000), which contain 24 muscle samples from patients with myosteatosis and 19 muscle samples from individuals without steatosis. The downloaded platform and series matrix files were processed in the R software package. Unqualified data were converted and rejected, and qualified data were calibrated, standardized and $\log_2$ transformed.

Statistical analyses

Statistical analysis was performed using GraphPad Prism 8. In *Figure* 1A and 1B, a two-tailed Student's *t*-test with Welch's correction was used, as indicated in the figure legend. 'n' represents the number of samples. In *Figure* 7, a one-way ANOVA followed with Dunnett's multiple comparison tests was used, as indicated in the figure legend. 'n' represents the number of image fields. Standard errors of mean were represented. NS, not significant. $^{*}P < 0.05$. $^{**}P < 0.01$. $^{***}P < 0.001$. All experiments in this study were replicated for at least three times with similar results obtained.

Virus production and infection

Adeno-associated virus (AAV) production and infection were performed using standard procedures.[14] AAV plasmids for knocking down *Ubr1* or *Ubr2* in mouse AML12 hepatocytes were generated from *AAV-TBG-gfp* (Addgene, 105535) by replacing the *gfp* sequence with the *U6* promoter followed by respective shRNA. Human HEK293T cells were transfected with AAV plasmids, Rep/Cap (2/8) plasmids and helper plasmids using polyethyleneimine (PEI) for AAV production and were harvested 48–60 h later for AAV purification. qPCR analysis was used to determine the titre of the purified virus. For knockdown of *Ubr1* and/or *Ubr2* in mouse AML12 hepatocytes, 1×10^6 cells were infected with AAV-TBG-*shgfp*, AAV-TBG-*shUbr1* and AAV-TBG-*shUbr2* at 2×10^8 or AAV-TBG-*shUbr1* and AAV-TBG-*shUbr2* each at 1×10^8 viral genome copies. In order to increase the basal lipid content in hepatocytes, 200 μM sodium oleate (Sigma-Aldrich, O7501) was added to the standard low-lipid containing culture medium 24 h before fixation.

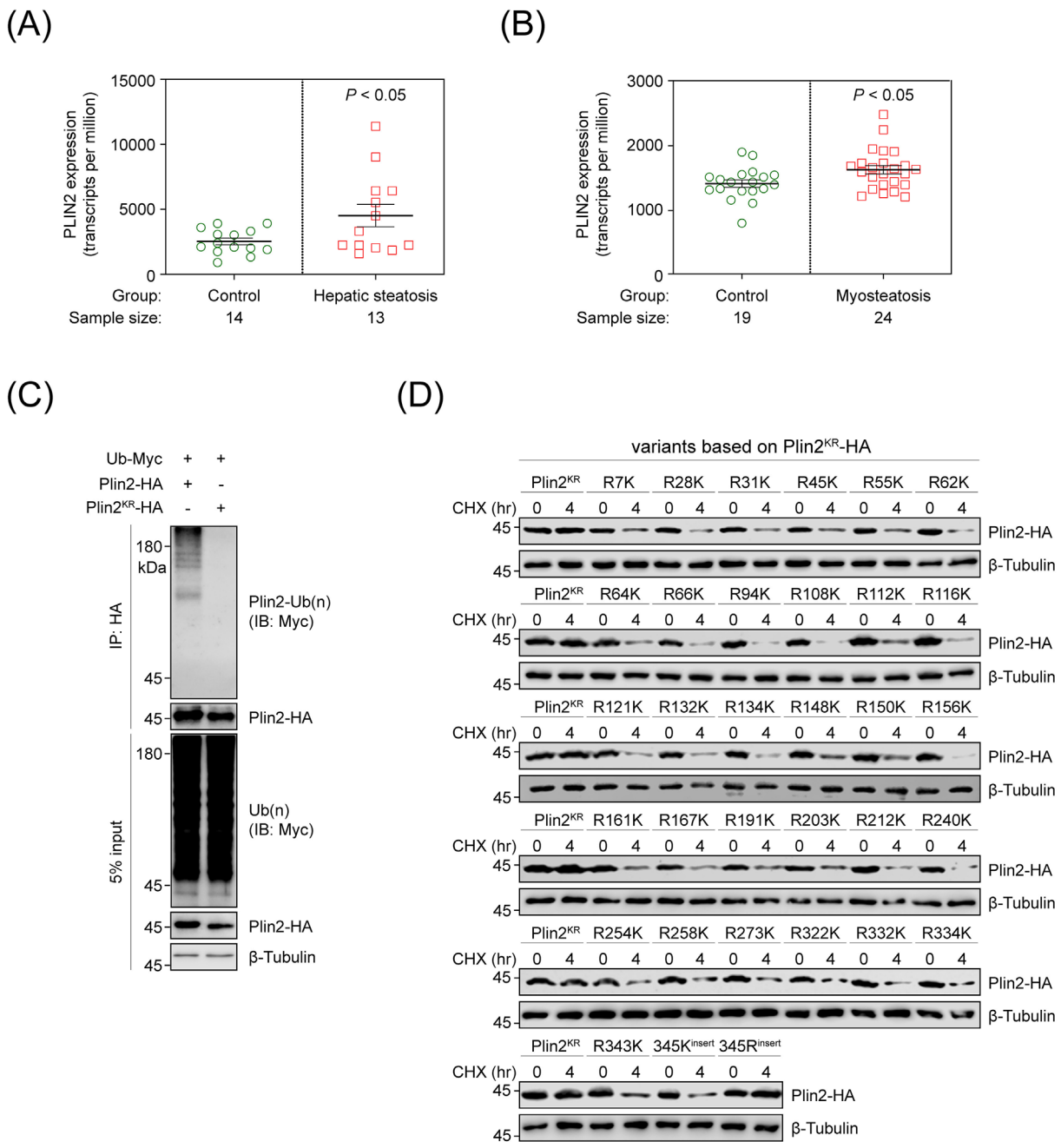

Figure 1 Patients with hepatic steatosis (hepatic steatosis group, n = 13) had significant higher expression of hepatic *PLIN2* compared to individuals without steatosis (control group, n = 14). $P < 0.05$. Two-tailed Student's t-test with Welch's correction (A). Compared with individuals without steatosis (control group, n = 19), the expression of *PLIN2* in patients with myosteatosis (myosteatosis group, n = 24) was significantly increased. $P < 0.05$. Two-tailed Student's t-test with Welch's correction (B). $Plin2^{KR}$, which was not modified by ubiquitination (C), displayed an extended half-life of more than 4 h (D). An Arg scan on Plin2 was performed to identify crucial Lys residues for Ub conjugation. Thirty mutants were constructed based on $Plin2^{KR}$, with a single mutated Lys residue changed back. The protein stability of $Plin2^{KR}$ was reduced when any mutated Lys residues were changed back. For R345K, a local Arg residue at 345 was replaced with Lys. For $353K^{insert}$ and $353R^{insert}$, a single Lys or Arg residue was inserted before the C-terminally tagged HA (D).

For infection of human JHH-7 and SNU-475 hepatoma cells, lentiviruses were packaged in HEK293T cells using standard procedures.[14] HEK293T cells were transfected with *TRC2-pLKO*, *pMD2G* and *psPAX2* plasmids. Seventy-two hours after transfection, conditioned media were collected and added to target cells for infection. After 48 h, cells were incubated with DMEM medium containing 15 mg/mL puromycin (Sigma-Aldrich, 540411) for selection prior to harvest.

DOI: 10.1002/jcsm.13233

Results

PLIN2 expression increases in patients with steatosis

Plin2, a LD protein that inhibits lipolysis,[22] has been considered as a causative factor of steatosis in liver and muscle.[23,24] Elevated Plin2 levels have also been observed in various animal models with hepatic steatosis or myosteatosis, independent of the original cause.[4,25,26] However, evidence supporting this correlation is lacking in humans.

To investigate whether this is the case, we analysed the mRNA levels of *PLIN2* in individuals with or without steatosis. The expression profiles of GSE138312 and GSE167186 were downloaded from the Gene Expression Omnibus (GEO) database.[20,21] The GSE138312 contains 27 liver samples, 13 from patients with hepatic steatosis and 14 from individuals without steatosis. The GSE167186 includes 43 muscle samples, 24 from patients with myosteatosis and 19 from individuals without steatosis. We analysed these data and found a significant increase in *PLIN2* expression in patients with steatosis in liver ($P < 0.05$) (*Figure* 1A) and muscle ($P < 0.05$) (*Figure* 1B). These data indicate that *PLIN2* is a risk factor of hepatic steatosis and myosteatosis. Of note, species-specific nomenclature for genes and proteins from representative backgrounds will be used throughout the manuscript (e.g. human: *PLIN2*, PLIN2; mouse: *Plin2*, Plin2; *Drosophila*: *plin2*, Plin2).

Plin2 is closely monitored by the ubiquitin–proteasome system

Since PLIN2 is closely associated with steatosis in humans (*Figure* 1A and 1B), uncovering the regulatory mechanisms of PLIN2 will aid in the diagnosis, prevention and treatment of steatosis. Our previous study has shown that wild-type Plin2 is a short-lived protein with a half-life of approximately 2 h and that ubiquitin modification is the main trigger for Plin2 degradation.[14]

Ubiquitin is covalently conjugated to lysyl amino groups of substrate proteins.[27] When all Lys residues in the Plin2 protein were mutated to Arg residues ($Plin2^{KR}$), the poly-ubiquitination modification was completely abolished (*Figure* 1C). Consistently, $Plin2^{KR}$ became more stable with a half-life of more than 4 h (*Figure* 1D).

To identify the key Lys residues responsible for Plin2 ubiquitination and subsequent degradation, we performed additional rounds of reverse mutagenesis of $Plin2^{KR}$ and examined the protein stability of $Plin2^{KR}$ revertants in cultured fly Schneider 2 (S2) cells (*Figure* 1D). We found that the ubiquitin moiety could be conjugated to any Lys residue in Plin2, as the $Plin2^{KR}$ protein became unstable when any mutated Lys residues reverted to Lys (*Figure* 1D). The same was true when the wild-type Arg residue in the $Plin2^{KR}$ mutant was replaced by Lys (R343K), which provided an ectopic site for ubiquitin modification (*Figure* 1D). This conclusion was further supported by the finding that insertion of an additional Lys ($345K^{insert}$) but not Arg residue to $Plin2^{KR}$ ($345R^{insert}$) effectively reduced the stability of the $Plin2^{KR}$ protein (*Figure* 1D). This phenomenon is not unprecedented, as similar findings have been reported for the ubiquitination of T cell antigen receptors and cyclin B,[28,29] which must be tightly regulated to prevent immune disease and tumorigenesis. Therefore, this seemingly nonspecific property would ensure timely degradation of Plin2 protein to prevent steatosis, highlighting the role of the ubiquitin–proteasome machinery in closely monitoring Plin2 protein homeostasis.

Ubr1 is an amino acid-activated negative regulator of steatosis

The Gal4/UAS system is commonly used in *Drosophila* to drive expression of RNAi or genes of interest.[30] Leveraging this powerful genetic tool, we used *Drosophila* wing imaginal disc as an in vivo model to study the pervasive regulatory mechanisms of Plin2 proteostasis and LD homeostasis. Upon expression by the dorsal-specific *ap*-Gal4 driver, genes of interest, including *white* (*w*), *Ubr1* and *Ubc6*, were individually knocked down by RNAi in the RFP-labelled region (*Figure* 2A). As a negative control, knockdown of *w* did not affect the protein levels of Plin2 (*Figure* 2A), as visualized by two in-frame YFP protein trap lines (CPTI-002546 and CPTI-001655). In contrast, knocking down *Ubr1*, or its cognate E2 conjugating enzyme *Ubc6*,[31] independently led to increased protein levels of Plin2 (*Figure* 2A). Note that the transgenic RNAi fly lines used in these experiments worked well, as verified by *in situ* hybridization using RNA probes targeting *Ubr1* and *Ubc6*, respectively (*Figure* 2A).

Since Plin2 acts as a positive regulator of LD stabilization, we hypothesized that inhibition of Ubr1-mediated Plin2 degradation may lead to excessive LD accumulation, a hallmark of steatosis. Indeed, upon knocking down either *Ubr1* or *Ubc6*, a substantial accumulation of LDs in RFP-positive dorsal regions was independently observed (*Figure* 2B). These data suggest that Ubr1 is a negative regulator of steatosis.

Our previous data showed that amino acids can activate Ubr1-mediated degradation of Plin2, indicating that Ubr1 may serve as an amino acid-responsive regulator of steatosis. To test this hypothesis, we performed immunoprecipitation to examine the activity of Ubr1 under different nutritional conditions. In these assays, the Ubr1–Plin2 interaction mirrors the activity of Ubr1. Of note, Plin2 was maintained at comparable protein levels in cells cultured in medium containing the proteasome inhibitor MG132. Consistent with our hypothesis, Ubr1 activity was inhibited under amino acid

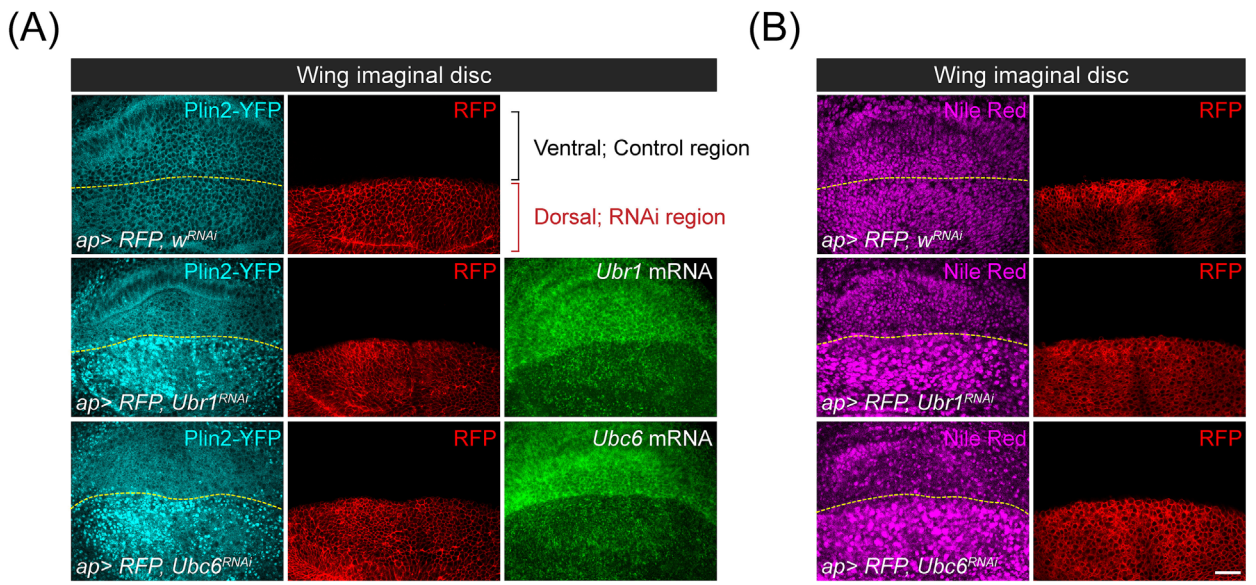

Figure 2 Ubr1 and Ubc6 are negative regulators of Plin2 proteostasis and LD homeostasis. Upon driven by *ap*-Gal4, *w*, *Ubr1* and *Ubc6* were independently knocked down by RNAi in RFP-positive dorsal regions, but not in RFP-negative ventral regions in *Drosophila* wing imaginal discs (A). Knockdown of either *Ubr1* or *Ubc6* led to increased Plin2, as visualized by Plin2-YFP (A), and LD accumulation as stained by Nile red (B). *w* was used as a negative control. Note that the efficacy of transgenic RNAi fly lines was measured by *in situ* hybridization using specific RNA probes for *Ubr1* and *Ubc6*, respectively (A). Scale bar, 10 μm.

starvation conditions (*Figure* 3A). This regulation was reversible, as Ubr1 was reactivated upon refeeding with standard medium (*Figure* 3A). Moreover, amino acid supplementation in ice-cold detergent-extracted lysates from amino acid-starved cells was also sufficient to reactivate Ubr1 (*Figure* 3B), suggesting that amino acids activate Ubr1 independent of enzymatic events, but more likely in a direct manner.

To address this hypothesis, we purified Ubr1 and FLAG-Plin2 proteins from HEK293 cells and reconstituted an in vitro cell-free system. Indeed, in the in vitro pulldown assay, Ubr1 was activated to bind to Plin2 only in the presence of amino acids (*Figure* 3C). Consistently, supplementing amino acids effectively promoted Ubr1-mediated Plin2 ubiquitination in the in vitro ubiquitination assay (*Figure* 3D), strongly indicating that Ubr1 regulates Plin2 proteostasis and LD homeostasis in an amino acid-activated manner.

Ubr1 is an amino acid sensor with two independent amino acid-binding pockets

Since amino acids can activate Ubr1 in vitro (*Figure* 3C and 3D), we hypothesized that these amino acids could directly bind to Ubr1. Previous studies have shown that type 1 (Arg, His and Lys) and type 2 N-terminal amino acid residues (Ile, Leu, Phe, Trp and Tyr) of protein substrates bind to the UBR-box-1 domain and UBR-box-2 domain in Ubr1, respectively.[11,32] Considering the structural similarity between N-terminal amino acid residues and free amino acids, we postulated that free amino acids may bind to the UBR-box-1/2 domains of Ubr1. Indeed, type 1 (Lys) and type 2 (Leu) amino acids immobilized on Silica MagBeads (*Figure* 4(A)) efficiently pulled down both purified Ubr1 protein (*Figure* 4B, upper panel) and endogenous Ubr1 from starved S2 cell lysates (*Figure* 4B, lower panel), with type 2 (Leu) beads being more efficient than type 1 (Lys) beads.

Binding of bead-bound type 1 amino acids to Ubr1 could be competed off by excess amount of unbound type 1 but not type 2 amino acids (*Figure* 4A and 4B) and vice versa. The above results suggest that these two amino acid-binding sites may function independently of each other. Consistent with this prediction, Ubr1 point mutants,[11] previously shown to block either type 1 ($Ubr1^{G157D}$ and $Ubr1^{D160E}$) or type 2 ($Ubr1^{D244N}$ and $Ubr1^{H247Y}$) N-terminal amino acid residue binding, were not pulled down with bead-bound type 1 or type 2 amino acids (*Figure* 4C). These results highlight the specific and independent binding of type 1 and type 2 sites with their correspondent amino acids.

Since Ubr1 uses different domains for type 1 and type 2 amino acid binding, we hypothesized that these two types of amino acids could activate Ubr1 independently of each other. Consistent with this hypothesis, the single-site Ubr1 mutants (*Figure* 4C) were still able to bind to Plin2 in S2 cells fed on complete medium, highlighting the independent roles of type 1 and type 2 amino acids in Ubr1 activation (*Figure* 4D, upper panel). As a control, the double-site mutants ($Ubr1^{G157D,\ D244N}$ and $Ubr1^{D160E,\ H247Y}$) (*Figure* 4C) did not bind to Plin2 (*Figure* 4D, upper panel). In starved S2 cells, type 1 mutants ($Ubr1^{G157D}$ or $Ubr1^{D160E}$) did not interact with Plin2 unless type 2 amino acids, such as Leu, were added to

DOI: 10.1002/jcsm.13233

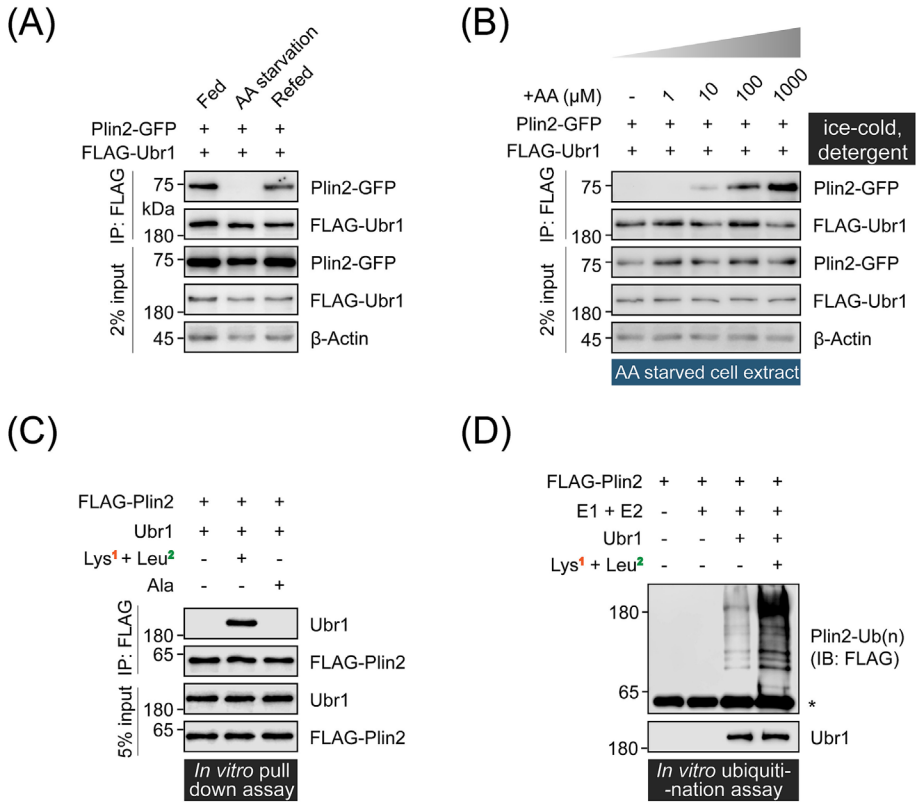

Figure 3 Amino acids activate Ubr1 to bind to and ubiquitylate Plin2. When S2 cells were depleted of amino acids in KRB buffer (AA starvation), Ubr1 did not bind to Plin2, and this interaction was restored when amino acid starved cells were refed with complete Schneider's medium (A). Amino acids were added to ice-cold, detergent-extracted cell lysate at the indicated concentrations. Ubr1-Plin2 interaction increased in a dose-dependent manner with increasing amino acid concentration (B). Purified Ubr1 failed to pull down FLAG-Plin2 in an in vitro cell-free system unless supplemented with type 1 (Lys) and type 2 amino acids (Leu) (C). Ala served as a negative control (C). Amino acids activated Ubr1 to ubiquitylate Plin2 in vitro. Purified FLAG-Plin2 protein was incubated with ubiquitin, UBE1 (E1), HR2B (E2) and Ubr1. Asterisk represents FLAG-Plin2 (D). For (C) and (D), Lys, Leu or Ala was added to a final concentration of 1 mM.

ice-cold cell lysates (*Figure* 4D, lower panel); type 2 mutants ($Ubr1^{D244N}$ and $Ubr1^{H247Y}$) bound to Plin2 only when supplemented with type 1 amino acids, such as Lys (*Figure* 4D, lower panel). Taken together, the data presented so far highlight Ubr1 as an amino acid sensor that contains two independent amino acid-binding pockets.

Amino acid binding activates Ubr1 by alleviating its auto-inhibition

Next, we focused on the mechanism by which amino acid binding activates Ubr1. Previous studies have shown that the C-terminal region of Ubr1 acts as an auto-inhibitory domain,[33] and our published data showed that the Plin2-binding domain is located in the internal region of Ubr1.[14] We therefore hypothesized that the C-terminal auto-inhibitory domain could inactivate Ubr1 by disrupting the access of Plin2 to its binding site. To test this hypothesis, we generated a Ubr1 mutant ($Ubr1^{\Delta C}$, amino acids 1–1531) depleted of its C-terminal region and examined its Plin2-binding ability under different nutritional conditions. Consistent with our prediction, $Ubr1^{\Delta C}$ binds to Plin2 in an amino acid-independent manner, suggesting that the C-terminal auto-inhibitory domain plays a critical role in Ubr1 inactivation upon amino acid starvation.

A plausible explanation for amino acid-induced activation of Ubr1 might be that amino acid binding induces an allosteric conformational change in Ubr1, thereby alleviating its auto-inhibition. We tested this hypothesis in S2 cells by expressing Ubr1-C (amino acids 1532–1824) and Ubr1-N (amino acids 1–1031), containing the Plin2-binding site, under different feeding conditions. Consistent with our hypothesis, these two truncated versions of Ubr1 bound to each other only under amino acid starvation conditions (*Figure* 5A and 5B), and either refeeding with standard medium (*Figure* 5A) or adding amino acids to cell lysates prevented binding (*Figure* 5B). Moreover, the interaction between Ubr1-N and Ubr1-C occurred when the two amino acid-binding sites were mutated, under fed conditions (*Figure* 5C, upper panel), or when the single binding site of the correspondent amino acid was mutated, under starved conditions (*Figure* 5C, lower panel);

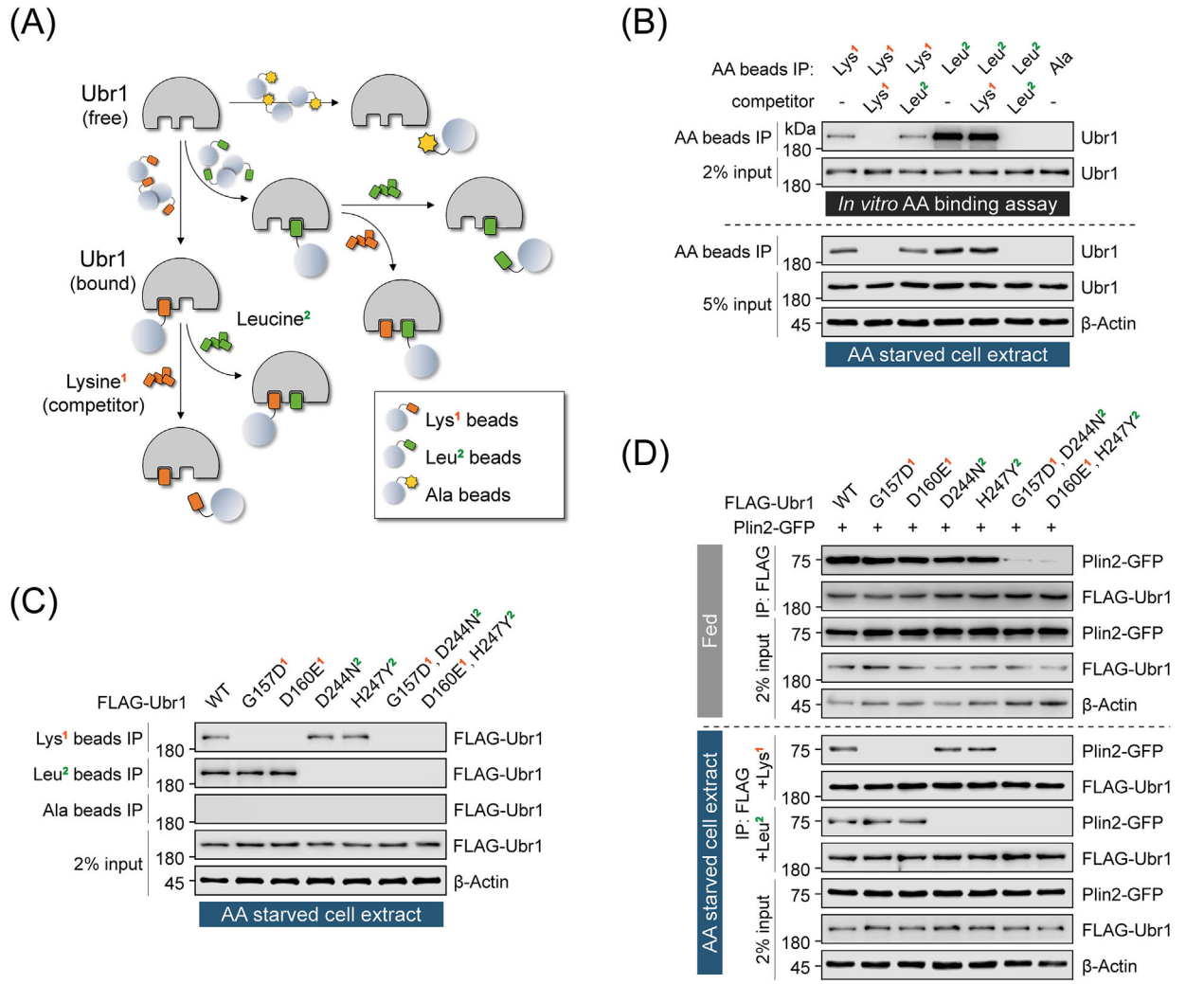

Figure 4 Ubr1 is an amino acid sensor. A schematic of the amino acid-binding assay of Ubr1 is shown in (A). Lys (type 1, orange)-immobilized, Leu (type 2, green)-immobilized or Ala (yellow)-immobilized beads were used to enrich for Ubr1 protein. Non-conjugated free amino acids were used as competitors (A). Purified Ubr1 protein (upper panel) or amino acid starved cell extract (lower panel) were incubated with Lys (type 1, orange), Leu (type 2, green) or Ala beads. Free Lys, Leu or Ala was added as indicated for competition (B). Ubr1 mutants defective in type 1 ($Ubr1^{G157D}$, $Ubr1^{D160E}$) or type 2 ($Ubr1^{D244N}$, $Ubr1^{H247Y}$) amino acid binding did not bind to correspondent amino acid beads. Note that type 1 Ubr1 mutants were still pulled down with type 2 amino acid beads, and vice versa (C). In fed S2 cells (D, upper panel), Ubr1 mutants lacking either type 1 or type 2 amino acid-binding capacity bound to Plin2, whereas Ubr1 double-site mutants ($Ubr1^{G157D,\ D244N}$, $Ubr1^{D160E,\ H247Y}$) did not. In starved S2 cells (D, lower panel), exogenous Lys (type 1) activated type 2, but not type 1 amino acid-binding defective Ubr1 mutants, whereas supplementation with Leu (type 2) activated type 1, but not type 2 amino acid-binding defective Ubr1 mutants. Double-site Ubr1 mutants remained inactive even upon addition of Lys or Leu (D).

in both circumstances, Ubr1 was unable to bind to Plin2 (Figure 4D). These results provide strong evidence that amino acid binding activates Ubr1 by alleviating its auto-inhibition.

Amino acid-activated PLIN2 degradation is evolutionarily conserved

To determine whether the amino acid-activated PLIN2 degradation is evolutionarily conserved, we performed co-immunoprecipitation to examine the activity of Ubr1 family proteins in cultured mammalian cells under different nutrient conditions. The proteasome inhibitor MG132 was used for experiments to inhibit Plin2/PLIN2 degradation. There are two orthologues of fly *Ubr1* in mice, namely, *Ubr1* and *Ubr2* (abbreviated as *Ubr1/2*), and two orthologues, namely, *UBR1* and *UBR2* (abbreviated as *UBR1/2*) in humans. Consistent with our observations in *Drosophila*, the binding between endogenous Ubr1/2 and Plin2 was eliminated in mouse AML12 normal hepatocytes upon amino acid starvation and was restored after refeeding (*Figure* 6A). Similar results were observed in hu-

DOI: 10.1002/jcsm.13233

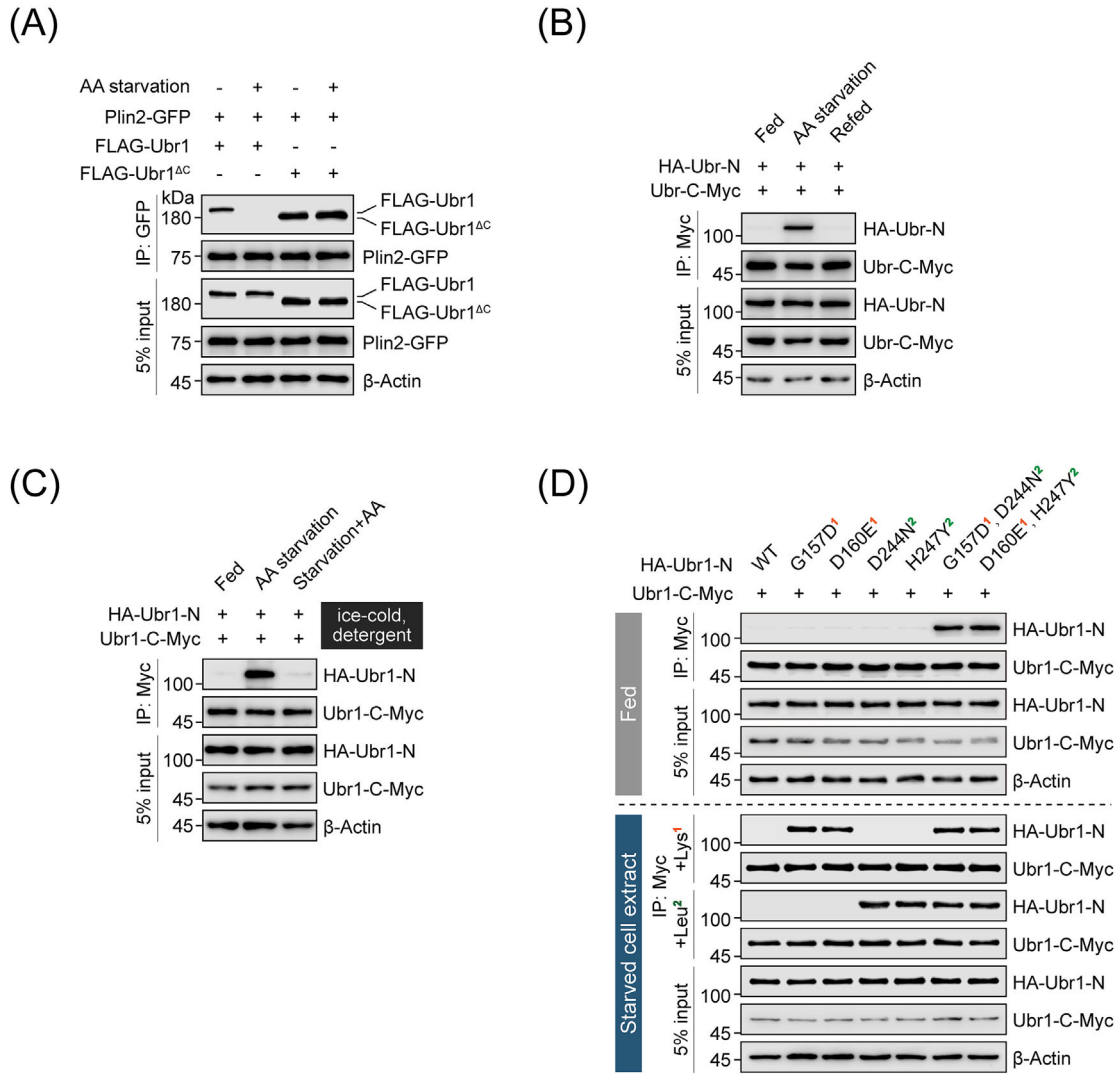

Figure 5 Amino acid binding activates Ubr1 by relieving its auto-inhibition. In S2 cells, the Ubr1-C deletion mutant Ubr1$^{\Delta C}$ (amino acids 1–1531) bound to Plin2 in an amino acid-independent manner (A). Interaction between Ubr1-N (amino acids 1–1031) and Ubr1-C (amino acids 1532–1824) was observed during amino acid deficiency (B and C), while refeeding cells with Schneider's medium (B) or adding amino acids to the lysate (C) suppressed this interaction. In fed S2 cells (D, upper panel), auto-inhibitory interactions were observed in double-site (Ubr1$^{G157D,\ D244N}$-N, Ubr1$^{D160E,\ H247Y}$-N), but not single-site Ubr1-N mutants (type 1, Ubr1^{G157D}-N and Ubr1^{D160E}-N; type 2, Ubr1^{D244N}-N and Ubr1^{H247Y}-N). In amino acid-starved cells (D, lower panel), exogenous Lys (type 1) prevented type 2, but not type 1 Ubr1-N mutants recognizing Ubr1-C. Similarly, addition of Leu (type 2) to cell lysate released the auto-inhibitory interaction of type 1, but not type 2 amino acid-binding defective Ubr1-N mutants. Neither Lys nor Leu affected auto-inhibition in double-site Ubr1-N mutants.

man JHH-7 and SNU-475 hepatoma cells. The above results demonstrate that UBR1/2 recognize endogenous PLIN2 in an amino acid-dependent manner (*Figure* 6B and 6C), highlighting that the amino acid-primed Ubr1 activity is evolutionarily conserved from flies to mammals.

Since both Ubr1 orthologues recognize Plin2/PLIN2 in mammalian cells (*Figure* 6A–C), we hypothesized that they may redundantly regulate Plin2/PLIN2 proteostasis. Indeed, knockdown of both *Ubr1/2*, but not *Ubr1* or *Ubr2* alone, increased protein levels of endogenous Plin2 in mouse AML12 normal hepatocytes (*Figure* 6D). Similarly, in human JHH-7 and SNU-475 hepatoma cells, a drastic increase of endogenous PLIN2 protein abundance was observed when *UBR1/2* were knocked down simultaneously, but not knocking down alone (*Figure* 6E and 6F). These data indicate that Ubr1 family proteins function redundantly to regulate Plin2 proteostasis in mammals.

Ubr1 family proteins prevent steatosis in an amino acid-dependent manner

To further investigate the role of Ubr1 family proteins in regulating lipid droplet homeostasis, we performed

DOI: 10.1002/jcsm.13233

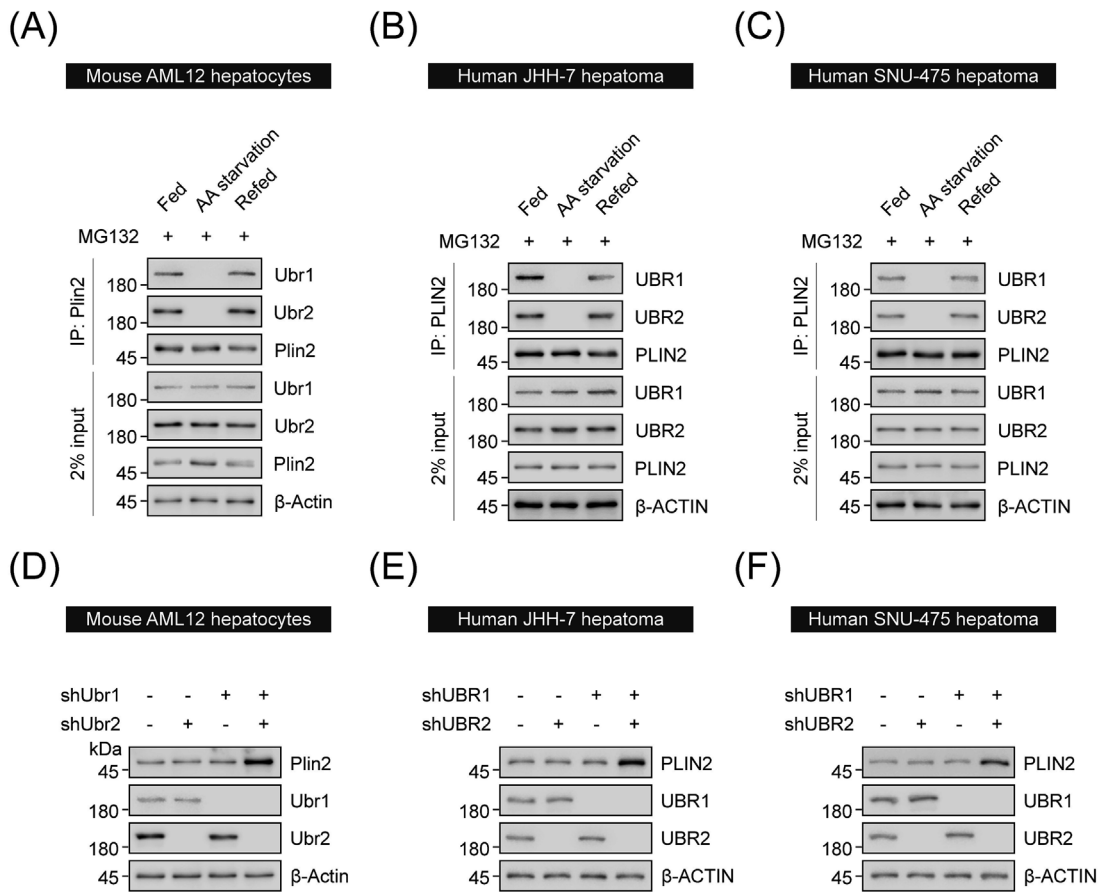

Figure 6 Amino acid-induced PLIN2 degradation is evolutionarily conserved. Endogenous mouse Ubr1/2 and human UBR1/2 specifically recognized endogenous Plin2/PLIN2 in an amino acid-dependent manner (A–C). Knockdown of both *Ubr1* and *Ubr2* (abbreviated as *Ubr1/2*) led to increased protein levels of endogenous Plin2 in mouse AML12 normal hepatocytes (D). In contrast, knocking down either *Ubr1* or *Ubr2* alone had no effects (D). Knocking down both human *UBR1* and *UBR2* (abbreviated as *UBR1/2*), but neither alone, stimulated protein levels of endogenous PLIN2 in human JHH-7 (E) and SNU-475 hepatoma cells (F). For (A), (B), and (C), MG132 was added to prevent PLIN2 degradation in the proteasome.

anti-Plin2 immunofluorescence and neutral lipid staining on mouse AML12 hepatocytes. Cells were treated with sodium oleate-containing medium to increase basal lipid content. The immunofluorescence results further confirmed the conclusion that Ubr1/2 function redundantly in regulating Plin2 proteostasis (*Figure* 7A). The upregulation of Plin2 resulted from simultaneous knockdown of *Ubr1/2* increased the lipid content in hepatocytes (*Figure* 7A).

Glucose serves as the major energy source, limiting basal lipolysis activity under normal feeding conditions.[14] Elevated lipolysis activity led to a decrease in lipid content in glucose-starved hepatocytes (*Figure* 7B). Knocking down both *Ubr1/2* almost completely prevented the reduction of lipid content caused by glucose starvation (*Figure* 7B). Consistent with the observation that amino acids are critical for Ubr1/2 activation, removal of amino acids from the culture medium antagonized the glucose starvation effect, which could not be further enhanced by additionally knocking down both *Ubr1/2* (*Figure* 7C; cf. 7B). These results highlight the important role of amino acid-activated PLIN2 degradation in protecting against steatosis in mammals.

Taken together, our study identified Ubr1 as an amino acid sensor of steatosis and unravelled a nutrient-sensing mechanism underlying the anti-steatosis effect of dietary amino acids. Therefore, our work provided potential strategies for the diagnosis, prevention and treatment of hepatic steatosis and myosteatosis.

Discussion

Steatosis contributes to the occurrence and development of many human metabolic diseases. For example, steatosis in skeletal muscles can lead to muscle atrophy and sarcopenia,[4,5] whereas hepatic steatosis can progress to NASH, cirrhosis and cancer.[34] To date, there are no

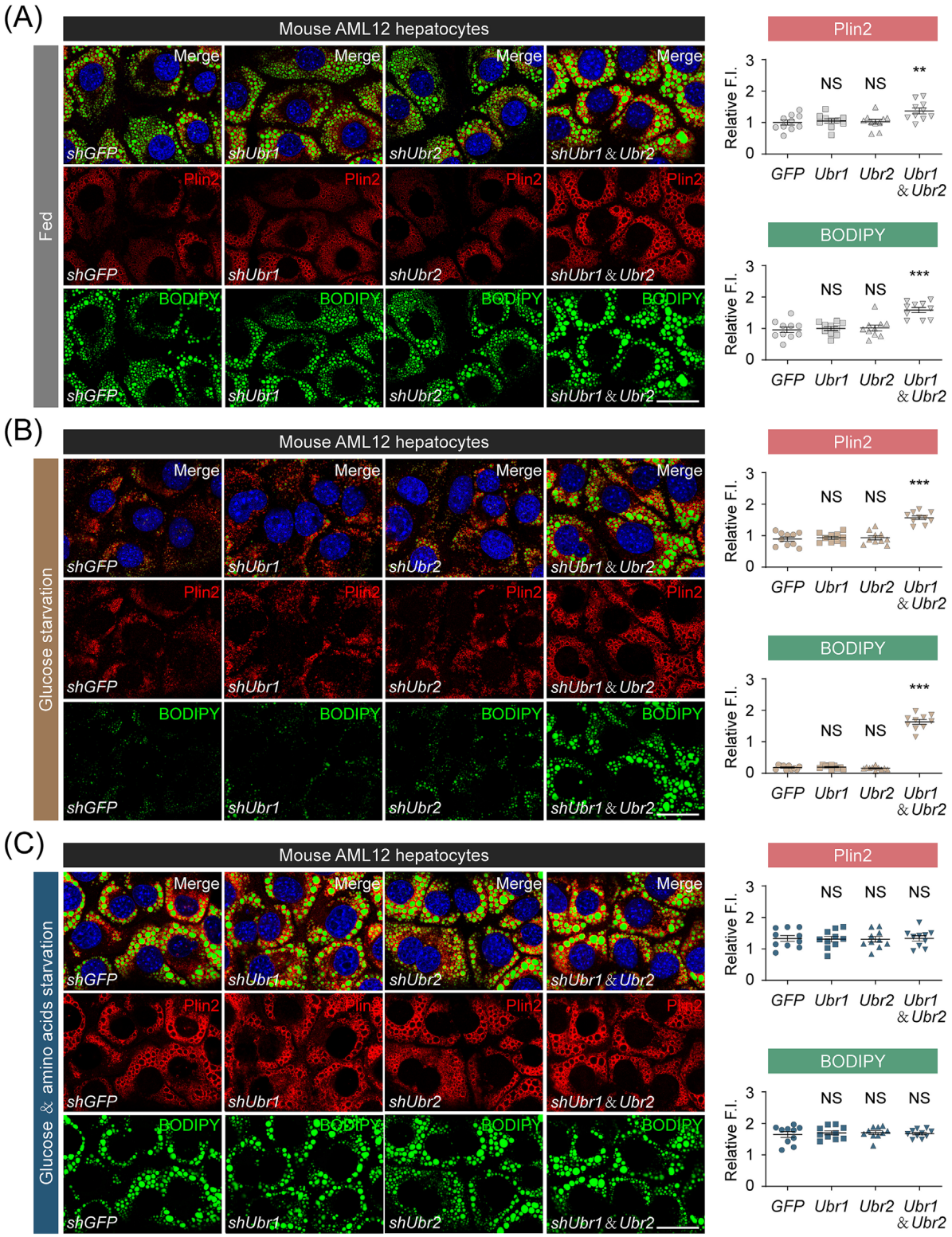

Figure 7 Ubr1 family proteins protect against steatosis in an amino acid-dependent manner. Adeno-associated virus (AAV)-mediated simultaneous knockdown of *Ubr1/2*, but neither alone, led to an increase in endogenous Plin2 and lipid content in mouse AML12 hepatocytes (A). The effect of knocking down Ubr1/2 was more pronounced in glucose-starved hepatocytes (B). Removal of amino acids from the culture medium was sufficient to block lipolysis induced by glucose starvation (C, cf. B). Neutral lipids (green) and chromatin (blue) were respectively stained by BODIPY and DAPI. In all experiments, the relative fluorescence intensity (FI) of Plin2 or BODIPY in mouse hepatocytes was normalized to the control group as shown in (A). *n* = 10, one-way ANOVA, Dunnett's multiple comparison tests.

DOI: 10.1002/jcsm.13233

FDA-approved pharmacological agents available for the treatment of steatosis. High-protein diets hold promise for steatosis treatment in common clinical practice.[35,36] A prospective study showed that a high-protein diet, independent of the protein source, reduced liver fat by 36–48% in patients with hepatic steatosis within 6 weeks.[37] Undoubtedly, understanding the underlying mechanisms will greatly facilitate the development of steatosis treatment strategies. Here, our identification of Ubr1 as an amino acid sensor for steatosis fills this knowledge gap, as increased protein intake provides free amino acids required for Ubr1 activation, leading to decreased protein levels of PLIN2 and reduced lipid content. Based on our results, we suggest that amino acid supplementation may be beneficial in reverting hepatic steatosis and myosteatosis, especially in patients with protein malnutrition.

Understanding the pathogenesis is a prerequisite for developing a disease treatment strategy. Identification of amino acid-induced Ubr1 activity in regulating lipid homeostasis suggests a strategy for the treatment of myosteatosis, a metabolic disorder strongly associated with sarcopenia. The development of small molecules with high affinity and specificity for Ubr1 activation may offer exciting therapeutic potential for simple intramuscular injections to reduce muscle lipid deposition, ameliorate loss of muscle mass and improve muscle function and quality. Further structural studies on the molecular mechanisms by which amino acids trigger Ubr1 activation will shed light on the design of Ubr1-targeting drugs.

Acknowledgements

We thank BDSC, VDRC and the TRiP at Tsinghua University for fly stocks and reagents. We also thank the National Center for Protein Science at Peking University, particularly Drs Guilan Li and Chunyan Shan, for assistance with short hairpin RNA (shRNA) library and microscopic imaging. This work was supported by the National Natural Science Foundation of China (31830058 to A.J.Z., 32170716 to M.L. and 81900431 to W.Z.), National Key Research and Development Program of China (2021YFA0805800 to A.J.Z. and M.L. and 2022YFC2009600 to W.Z.), Qidong-SLS Innovation Fund (to A.J.Z.) and Beijing Hospitals Authority Youth Programme (QML20210702 to W.Z.). The authors of this manuscript certify that they comply with the ethical guidelines for authorship and publishing in the *Journal of Cachexia, Sarcopenia and Muscle*.[38]

Conflict of interest

All authors declare that they have no conflicts of interest.

Online supplementary material

Additional supporting information may be found online in the Supporting Information section at the end of the article.

References

1. Chantranupong L, Wolfson RL, Sabatini DM. Nutrient-sensing mechanisms across evolution. *Cell* 2015;**161**:67–83.
2. Efeyan A, Comb WC, Sabatini DM. Nutrient-sensing mechanisms and pathways. *Nature* 2015;**517**:302–310.
3. Friedman SL, Neuschwander-Tetri BA, Rinella M, Sanyal AJ. Mechanisms of NAFLD development and therapeutic strategies. *Nat Med* 2018;**24**:908–922.
4. Yan Y, Wang H, Hu M, Jiang L, Wang Y, Liu P, et al. HDAC6 suppresses age-dependent ectopic fat accumulation by maintaining the proteostasis of PLIN2 in *Drosophila*. *Dev Cell* 2017;**43**:99–111.e5.
5. Katewa SD, Demontis F, Kolipinski M, Hubbard A, Gill MS, Perrimon N, et al. Intramyocellular fatty-acid metabolism plays a critical role in mediating responses to dietary restriction in *Drosophila melanogaster*. *Cell Metab* 2012;**16**:97–103.
6. Williams CD. A nutritional disease of childhood associated with a maize diet. *Arch Dis Child* 1933;**8**:423–433.
7. Liebe R, Esposito I, Bock HH, Vom Dahl S, Stindt J, Baumann U, et al. Diagnosis and management of secondary causes of steatohepatitis. *J Hepatol* 2021;**74**:1455–1471.
8. Sakada M, Tanaka A, Ohta D, Takayanagi M, Kodama T, Suzuki K, et al. Severe steatosis resulted from anorexia nervosa leading to fatal hepatic failure. *J Gastroenterol* 2006;**41**:714–715.
9. Bartel B, Wünning I, Varshavsky A. The recognition component of the N-end rule pathway. *EMBO J* 1990;**9**:3179–3189.
10. Pan M, Zheng Q, Wang T, Liang L, Mao J, Zuo C, et al. Structural insights into Ubr1-mediated N-degron polyubiquitination. *Nature* 2021;**600**:334–338.
11. Varshavsky A. N-degron and C-degron pathways of protein degradation. *Proc Natl Acad Sci U S A* 2019;**116**:358–366.
12. Xia Z, Webster A, Du F, Piatkov K, Ghislain M, Varshavsky A. Substrate-binding sites of UBR1, the ubiquitin ligase of the N-end rule pathway. *J Biol Chem* 2008;**283**:24011–24028.
13. Sherpa D, Chrustowicz J, Schulman BA. How the ends signal the end: Regulation by E3 ubiquitin ligases recognizing protein termini. *Mol Cell* 2022;**82**:1424–1438.
14. Zhang Y, Lin S, Peng J, Liang X, Yang Q, Bai X, et al. Amelioration of hepatic steatosis by dietary essential amino acid-induced ubiquitination. *Mol Cell* 2022;**82**:1528–1542.e10.
15. Kume K, Iizumi Y, Shimada M, Ito Y, Kishi T, Yamaguchi Y, et al. Role of N-end rule ubiquitin ligases UBR1 and UBR2 in regulating the leucine-mTOR signaling pathway. *Genes Cells* 2010;**15**:339–349.
16. Liu M, Liu A, Wang J, Zhang Y, Li Y, Su Y, et al. Competition between two phosphatases fine-tunes Hedgehog signaling. *J Cell Biol* 2021;**220**:e202010078.
17. Aguilera-Gomez A, van Oorschot MM, Veenendaal T, Rabouille C. In vivo vizualisation of mono-ADP-ribosylation by dPARP16 upon amino-acid starvation. *Elife* 2016;**5**:e21475.
18. Jiang Y, Liu T, Lee CH, Chang Q, Yang J, Zhang Z. The NAD^+-mediated self-inhibition mechanism of pro-neurodegenerative SARM1. *Nature* 2020;**588**:658–663.
19. Grönke S, Beller M, Fellert S, Ramakrishnan H, Jäckle H, Kühnlein RP. Control of fat storage by a *Drosophila* PAT domain protein. *Curr Biol* 2003;**13**:603–606.

20. Barrett T, Wilhite SE, Ledoux P, Evangelista C, Kim IF, Tomashevsky M, et al. NCBI GEO: archive for functional genomics data sets--update. *Nucleic Acids Res* 2013;**41**: D991–D995.
21. Edgar R, Domrachev M, Lash AE. Gene Expression Omnibus: NCBI gene expression and hybridization array data repository. *Nucleic Acids Res* 2002;**30**: 207–210.
22. Listenberger LL, Ostermeyer-Fay AG, Goldberg EB, Brown WJ, Brown DA. Adipocyte differentiation-related protein reduces the lipid droplet association of adipose triglyceride lipase and slows triacylglycerol turnover. *J Lipid Res* 2007;**48**: 2751–2761.
23. Chang BH, Li L, Paul A, Taniguchi S, Nannegari V, Heird WC, et al. Protection against fatty liver but normal adipogenesis in mice lacking adipose differentiation-related protein. *Mol Cell Biol* 2006;**26**: 1063–1076.
24. Chang BH, Li L, Saha P, Chan L. Absence of adipose differentiation related protein upregulates hepatic VLDL secretion, relieves hepatosteatosis, and improves whole body insulin resistance in leptin-deficient mice. *J Lipid Res* 2010;**51**:2132–2142.
25. Su W, Wang Y, Jia X, Wu W, Li L, Tian X, et al. Comparative proteomic study reveals 17β-HSD13 as a pathogenic protein in non-alcoholic fatty liver disease. *Proc Natl Acad Sci U S A* 2014;**111**:11437–11442.
26. Imai Y, Varela GM, Jackson MB, Graham MJ, Crooke RM, Ahima RS. Reduction of hepatosteatosis and lipid levels by an adipose differentiation-related protein antisense oligonucleotide. *Gastroenterology* 2007;**132**:1947–1954.
27. Collins GA, Goldberg AL. The logic of the 26S proteasome. *Cell* 2017;**169**: 792–806.
28. Hou D, Cenciarelli C, Jensen JP, Nguygen HB, Weissman AM. Activation-dependent ubiquitination of a T cell antigen receptor subunit on multiple intracellular lysines. *J Biol Chem* 1994;**269**:14244–14247.
29. King RW, Glotzer M, Kirschner MW. Mutagenic analysis of the destruction signal of mitotic cyclins and structural characterization of ubiquitinated intermediates. *Mol Biol Cell* 1996;**7**:1343–1357.
30. Brand AH, Perrimon N. Targeted gene expression as a means of altering cell fates and generating dominant phenotypes. *Development* 1993;**118**:401–415.
31. Dohmen RJ, Madura K, Bartel B, Varshavsky A. The N-end rule is mediated by the UBC2 (RAD6) ubiquitin-conjugating enzyme. *Proc Natl Acad Sci U S A* 1991;**88**:7351–7355.
32. Matta-Camacho E, Kozlov G, Li FF, Gehring K. Structural basis of substrate recognition and specificity in the N-end rule pathway. *Nat Struct Mol Biol* 2010; **17**:1182–1187.
33. Du F, Navarro-Garcia F, Xia Z, Tasaki T, Varshavsky A. Pairs of dipeptides synergistically activate the binding of substrate by ubiquitin ligase through dissociation of its autoinhibitory domain. *Proc Natl Acad Sci U S A* 2002;**99**:14110–14115.
34. Younossi Z, Anstee QM, Marietti M, Hardy T, Henry L, Eslam M, et al. Global burden of NAFLD and NASH: trends, predictions, risk factors and prevention. *Nat Rev Gastroenterol Hepatol* 2018;**15**:11–20.
35. El-Agroudy NN, Kurzbach A, Rodionov RN, O'Sullivan J, Roden M, Birkenfeld AL, et al. Are lifestyle therapies effective for NAFLD treatment? *Trends Endocrinol Metab* 2019;**30**:701–709.
36. Eslam M, George J. Genetic insights for drug development in NAFLD. *Trends Pharmacol Sci* 2019;**40**:506–516.
37. Markova M, Pivovarova O, Hornemann S, Sucher S, Frahnow T, Wegner K, et al. Isocaloric diets high in animal or plant protein reduce liver fat and inflammation in individuals with type 2 diabetes. *Gastroenterology* 2017;**152**:571–585.e8.
38. von Haehling S, Morley JE, Coats AJS, Anker SD. Ethical guidelines for publishing in the Journal of Cachexia, Sarcopenia and Muscle: update 2021. *J Cachexia Sarcopenia Muscle* 2021;**12**:2259–2261.